ACS Sustainable Chemistry & Engineering

Research Article

Cite This: ACS Sustainable Chem. Eng. 2019, 7, 16310−16319

pubs.acs.org/journal/ascecg

Ettringite-Related Dimensional Stability of CO_2-Cured Portland Cement Mortars

Duo Zhang, Victor C. Li, and Brian R. Ellis*

Department of Civil and Environmental Engineering, University of Michigan, 1351 Beal Avenue, EWRE, Ann Arbor, Michigan 48109, United States

ABSTRACT: Carbonation curing, where cement is cured in a CO_2-rich environment, is an emerging technology in the precast industry that promotes CO_2 sequestration in construction materials. It demonstrates good promise for enhancing material strength development, chemical resistance, and manufacturing sustainability. A critically important but little studied aspect of carbonation curing is the dimensional stability of the cured materials, which poses a significant impact on the longevity of cement-based materials and structures. In this study, we propose the use of carbonation curing, in place of conventional energy-intensive steam curing and time-consuming moisture curing, and examine the dimensional stability of Portland cement mortars manufactured by different curing approaches. The common pathology in precast concrete that potentially creates undesirable expansions, known as Delayed Ettringite Formation (DEF), is particularly investigated. Four curing approaches were examined including moist, steam (maximum temperature at 85 °C to purposefully induce DEF), combined steam-carbonation, and carbonation curing in which steam curing was used to verify favorable cement chemistry for DEF and to indicate DEF onset timing. It was found that, among the four curing approaches designed in this study, the carbonation-cured mortars demonstrated the lowest expansion (~0%) whereas the steam-cured mortars showed the highest (>0.6%) after 500 days of storage in saturated limewater. Mortar expansion after the combined steam-carbonation curing (~0.1%) was lower than that of steam curing but remained higher with respect to the moisture-cured reference. The mineral ettringite was detected at 500 days after all curing approaches. However, larger ettringite crystal size (5−10 μm) with greater dispersion was observed via scanning electron microscopy after steam curing in reference to carbonation curing (<5 μm). Additionally, the calcium carbonate precipitated by CO_2 carbonation was found to participate in the postcarbonation hydration to promote formation of monocarboaluminate and hemicarboaluminate, which stabilize ettringite and potentially lead to a secondary densification of the mortar microstructure.

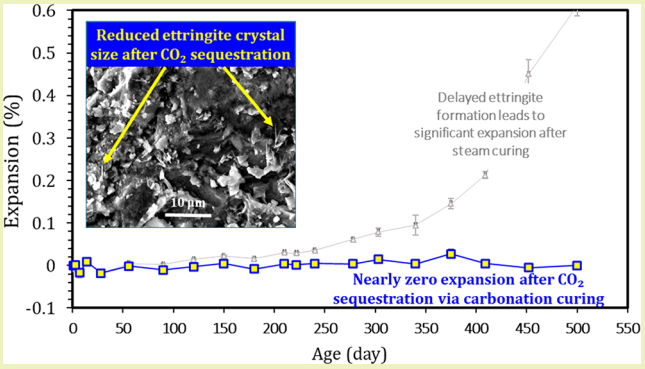

KEYWORDS: *Dimensional stability, Delayed ettringite formation, Carbonation curing, CO_2 sequestration, Cement*

INTRODUCTION

In precast applications of cement-based materials, curing is generally an indispensable process that ensures manufacturing efficiency and product performance. To facilitate Portland cement (PC) hydration and expedite early age strength gain, elevated temperature and high relative humidity are frequently adopted, hence forming the basis of the well-known "steam curing" at atmospheric pressure and "autoclave curing" at high pressures. Elevated temperatures, however, dissolve ettringite ($3CaO{\cdot}Al_2O_3{\cdot}3CaSO_4{\cdot}32H_2O$) at the early age,[1,2] but allow it to slowly reprecipitate after cooling down.[3,4] The rapidly formed C−S−H also binds free sulfate at the elevated temperature,[5] hence preventing ettringite formation at the early age, but releases sulfate over time for ettringite precipitation. The incompatibility between ettringite crystals and the microstructure of hardened cement paste creates tensile stress at the microscale that eventually leads to material swelling and cracking. This pathology in the chemistry of cement and concrete has been well recognized as "delayed ettringite formation (DEF)".[6]

The carbonation of matured concrete exposed to atmospheric conditions, known as weathering carbonation, is generally regarded as a cause of deterioration in PC-based concrete structures.[7] The alkaline environment created by PC hydration in pore solution is progressively neutralized during weathering carbonation, whereby decreasing pH enhances vulnerability to corrosion of the reinforcing steel. Severe carbonation can also lead to dissociation of calcium silicate hydrates (C−S−H),[8,9] thereby impairing the mechanical integrity of the hydrated PC paste.[10] Besides weathering carbonation, CO_2 carbonation of PC can also occur at the early hydration ages, when both hydrated and unhydrated phases of

Received: June 12, 2019
Revised: September 3, 2019
Published: September 5, 2019

DOI: 10.1021/acssuschemeng.9b03345
ACS Sustainable Chem. Eng. 2019, 7, 16310−16319

PC are equally and intentionally engaged in CO_2 carbonation. The primary reactions of early age carbonation are shown in eqs 1−4,[11,12] in which x and y vary with the degree of carbonation, and eq 3 is a general form of C−S−H carbonation with potentially varying stoichiometry. The rapid reactions occurring between calcium silicates and CO_2 (eqs 1 and 2) substantially expedite material strength gain, hence motivating the novel concept of using CO_2 as a curing agent, known as "CO_2/carbonation curing".[13] The precipitation of carbonation products also densifies PC's microstructure and leads to lower permeability and enhanced material durability.[14−17] Additionally, carbonation curing creates a novel strategy for permanent CO_2 sequestration by transforming waste CO_2 gas into solid, value-added products. Carbonation curing is generally completed within a few hours to several days and allows the unreacted cement to subsequently hydrate, thereby promoting secondary strength gain in the long term.[13,18] As carbonation curing is an early age process, the short-period CO_2 exposure does not damage material strength development as led by C−S−H dissociation during the long-term weathering carbonation.

$$3CaO{\cdot}SiO_2 + (3 - x)CO_2 + yH_2O \rightarrow xCaO{\cdot}SiO_2{\cdot}yH_2O + (3 - x)CaCO_3 \quad (1)$$

$$2CaO{\cdot}SiO_2 + (2 - x)CO_2 + yH_2O \rightarrow xCaO{\cdot}SiO_2{\cdot}yH_2O + (2 - x)CaCO_3 \quad (2)$$

$$3CaO{\cdot}2SiO_2{\cdot}3H_2O + 3CO_2 \rightarrow 3CaCO_3 + 2SiO_2 + 3H_2O \quad (3)$$

$$Ca(OH)_2 + CO_2 \rightarrow CaCO_3 + H_2O \quad (4)$$

In comparison to traditional steam, autoclave, or moist curing, carbonation curing demonstrates superior sustainability and economic performance. Specifically, the production of 1 m^3 concrete through steam and autoclave curing consumes 0.59 and 0.71 GJ, respectively, but it would consume only 0.013 GJ if carbonation curing were adopted by using industrial flue gas.[19,20] The expedited material strength development during carbonation curing has a manufacturing time that is comparable to that of steam curing, which shortens concrete productions from 1 to 7 d (by moist curing) to less than 1 d, with a CO_2 sequestration capacity of more than 10−20% by cement mass.[21,22] As carbonation curing is conducted in an enclosed static or flow-through environment, the residual CO_2 after reaction can be collected and recycled, leaving no uncontrollable CO_2 release during the process. Although technical and sustainable metrics could plausibly vary among specific products, carbonation curing clearly possesses a vast potential for reducing energy and carbon footprints, as well as enhancing manufacturing efficiency of the precast industry.

CO_2 carbonation can impact ettringite in several ways.[23,24] Equation 5 demonstrates the carbonation-induced ettringite decomposition on exposure to CO_2-rich environments, where ettringite dissolves followed by precipitation of calcium carbonate, gypsum, and alumina gel ($x \sim 3$).[25−27] Ettringite formation can also be promoted by CO_2 carbonation after exposure to the atmosphere. It was reported that CO_2 at a partial pressure of 0.5 kPa was sufficient to release SO_4^{2-} from monosulphoaluminate (Ms), hence favoring the formation of ettringite by supplying an additional source of sulfate.[28] In a similar manner, CO_3^{2-} dissolved from limestone in the widely used Ordinary Portland Cement (OPC) can substitute SO_4^{2-} in Ms to form monocarboaluminate (Mc), which further promotes SO_4^{2-} dissolution and DEF.[29,30] The low alkalinity of pore solution after CO_2 carbonation also leads to desorption of physically bound SO_4^{2-} from C−S−H.[23] Carbonation-induced dissociation of C−S−H potentially aggravates this desorption process and releases even more SO_4^{2-} for ettringite formation.

$$3CaO{\cdot}Al_2O_3{\cdot}3CaSO_4{\cdot}32H_2O + 3CO_2 \rightarrow 3CaCO_3 + CaSO_4{\cdot}2H_2O + Al_2O_3{\cdot}xH_2O + (26 - x)H_2O \quad (5)$$

Although carbonation has been well recognized to affect dissolution and formation of ettringite, possibly in a similar manner as the high temperature adopted for steam curing, previous studies have not investigated the evolution of ettringite and its impact on material stability in the unique context of early age carbonation curing. The lack of knowledge on ettringite formation after early age carbonation curing could potentially result in unexpected swelling and cracking that would lead to earlier structural deterioration and reduced service life. To clarify this impact, we present a laboratory experiment to examine expansion of PC-based mortar bars subjected to moist curing, steam curing at an excessively high temperature to trigger DEF, and carbonation curing. We also evaluated a new curing approach that combines steam curing and CO_2 carbonation. Length and mass of mortar specimens were recorded up to 500 days. Surface electrical resistivity, which serves as an indicator of surface permeability of the mortar bars, was measured over the same period. Phase assemblage and micromorphology were characterized with X-ray diffraction (XRD), thermogravimetric analysis (TGA), and scanning electron microscopy (SEM).

EXPERIMENTAL PROGRAM

Materials and Mix Proportion. Type I PC (chemical composition shown in Table 1), silica sand (conformed to ASTM C109), and deionized water were used for mortars. Water-to-cement (w/c) ratio was kept at 0.45, and cement-to-sand ratio was 1:2.5. A high range water reducer (HRWR) was added at 0.5% of the PC mass. The fresh mixture was cast into mortar bars with dimensions of 25 × 25 × 285 mm. Steel studs were preset at the two ends with an internal net distance of 254 mm.

Table 1. Chemical Composition of As-Received Cement As Measured via X-ray Fluorescence

Oxide	Quantity (%)
CaO	62.3
SiO_2	19.3
Al_2O_3	5.2
Fe_2O_3	2.6
MgO	2.5
SO_3	4.1
$Na_2O_{(eq)}$	0.96
Free CaO	0.9
LOI	2.3

The mixing protocol followed ASTM C305 using a 5-Qt. Hobart bench mixer. The mixing water and HRWR were premixed. Cement was added to the water and was mixed at low speed for 30 s, followed by the slow addition of sand over a period of 30 s without stopping the mixer. The mortar mixture was mixed at medium speed for an additional 30 s and was then stopped for 90 s. After manually scraping

DOI: 10.1021/acssuschemeng.9b03345
ACS Sustainable Chem. Eng. 2019, 7, 16310−16319

down the materials attached to the side of the mixer, the mortar mixture was mixed for an additional 60 s at a medium speed before molding.

Curing Regimes. Four curing regimes were considered, including moisture curing, steam curing (max. temp at 85 °C), combined steam (max. temp at 85 °C)-carbonation curing, and carbonation curing. All curing methods were finalized within 24 h after casting. The moisture curing was designed as a benchmark and was conducted by sealing fresh mortar bars within a plastic membrane immediately upon molding. The sealed mortars were stored in a moisture room for 24 h before demolding. Simultaneously, the other three groups of mortar bars were subjected to the curing regimes described as follows. Note that a high curing temperature (>70 °C) was adopted to trigger DEF in steam-cured mortars. This can also validate the favorable binder chemistry used in this experiment for the occurrence of DEF. Carbonation curing, however, does not need to be conducted at the same temperature as that of steam curing due to the different chemical mechanisms that may trigger DEF in CO_2-cured mortars.

Steam Curing. Steam curing was conducted in an environmental chamber with a programmed temperature profile as shown in Figure 1. The maximum curing temperature was chosen at 85 °C in order to

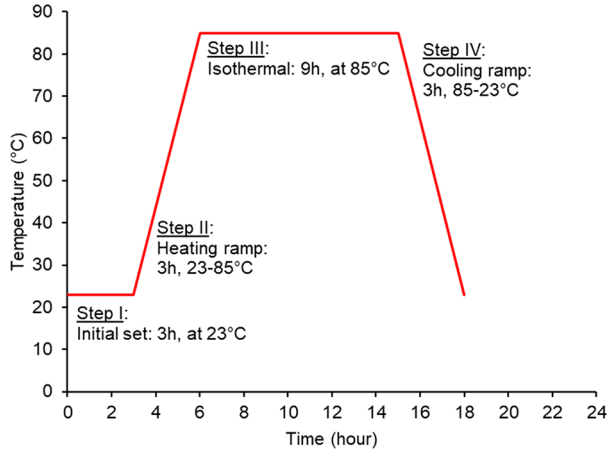

Figure 1. Steam curing temperature program comprises four steps: (1) initial set, (2) heating ramp, (3) isothermal process, and (4) cooling ramp. Steam curing is completed at 18 h after casting.

purposefully trigger DEF in the steam-cured mortars. The steam curing was composed of four steps: (1) initial set at 23 °C for 3 h, (2) heating ramp from 23 to 85 °C in 3 h, (3) hold at 85 °C for 9 h, and (4) cooling ramp from 85 to 23 °C in 3 h. The relative humidity (RH) was kept at 98% throughout the curing process to minimize water evaporation from the mortar bars. After the 18 h curing, mortar bars were sealed in a plastic bag awaiting initial length reading at 24 h.

Carbonation Curing. For carbonation curing, mortar bars were kept in air (T = 23 °C, RH = 50 ± 3%) after casting and molding. The mortar bars were demolded at the age of 14 h and were further dried for an additional 4 h using an electric fan. The purpose of sample drying is to not to fully dry the samples, but instead to evacuate sufficient porosity so as to allow faster diffusion of CO_2 gas into the mortar samples. After recording the precarbonation mass, the mortar bars were placed in a sealed plastic bag connected to CO_2 gas at atmospheric pressure. The plastic bag was vacuumed prior to being filled with pure CO_2 gas. Carbonation was conducted for 4 h during which CO_2 gas was manually replenished to promote continued reaction. After carbonation, the mortar bars were weighed and then sealed for additional 2 h prior to the initial length measurement at the age of 24 h. All mortar surfaces were exposed to CO_2 during carbonation. The carbonation front was determined using phenolphthalein indicator. The depth of carbonation was found to be 3−4 mm as shown in Figure 2.

Combined (Steam-Carbonation) Curing. The purpose of combining steam and carbonation curing was to assess the viability

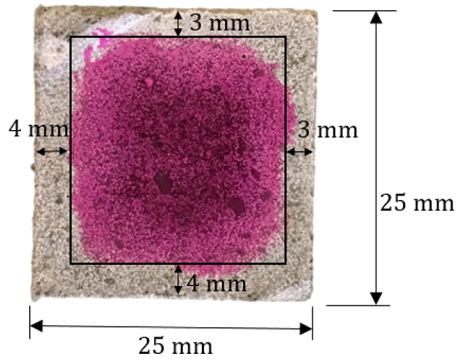

Figure 2. Phenolphthalein pH indicator sprayed on a cross-section of a carbonation-cured mortar bar.

of utilizing CO_2 to mitigate steam curing-induced DEF. This curing protocol combined a 4 h carbonation treatment of the mortar bars directly following steam curing. The mortar bars were first steam cured following the same protocol described in Steam curing and were then fan-dried for 2 h before exposure to CO_2. The mortar bars were carbonated for 4 h prior to initial length measurements at the age of 24 h.

Storing Condition and Mortar Bar Measurement. Physical measurements of mortar bars included mass, surface electrical resistivity (SER), and length. After initial measurements at 24 h, mortar bars were fully immersed in saturated limewater at room temperature (23 °C) until 500 d. At 28 d intervals through the 500 d experiment, the mortar bars were surface dried and measured following a sequence of SER, mass, and length. It is recognized that storage in limewater could slow down the leaching of alkali from PC hydration products, hence leading to a longer induction period for DEF to occur.[31] Nevertheless, the leachability of PC-based mortars is potentially altered after carbonation, which leads to inconsistent leaching behaviors between the carbonation-cured and noncarbonated specimens. As such, limewater was used to minimize the effect of leaching.

SER was investigated using a Proceq Resipod Resistivity Meter with four probes. The electric current induced from the outer two probes can be identified by the inner ones. The measurement was performed on four sides of each mortar bar and the average value was recorded. Following surface resistivity measurement, the mortar bars were weighed on a digital scale with a precision of 0.01 g. The purpose of measuring sample mass was to determine the moisture uptake in mortar, which is essentially linked to the long-term hydration and ettringite formation. Length of the mortar bars was measured with a comparator at a precision of 0.001 mm. All measurements were reported with respect to their initial readings at 24 h.

Water absorption was measured on mortar specimens after 500 d. Vacuum saturation was applied to achieve a complete saturation of air void and dead-end pores.[32] The saturated specimens were dried at two temperature levels, i.e., 60 and 105 °C, with a holding period of 24 h before each measurement. The standard temperature for concrete drying (ASTM C642) is 105 °C, whereas 60 °C was chosen to preserve the pore structure from damages associated with thermal decomposition of hydration products. Three specimens were measured with the average reported.

Characterization of DEF. At 500 d, mortar bars were cut to pieces smaller than 5 mm and were soaked in isopropanol to stop further hydration. After a 3 d isopropanol immersion, the samples were stored in a vacuum desiccator for an additional 7 d. The dried samples were ground and passed through a 75 μm sieve for thermogravimetric analysis (TGA) and through a 30 μm sieve for X-ray powder diffraction (XRD). A TA Instruments SDT650 model was used for TGA where, approximately, 10 mg of powdered sample was mounted in an alumina crucible and heated from room temperature to 1100 °C at a rate of 10 °C/min. The furnace was purged with pure

DOI: 10.1021/acssuschemeng.9b03345
ACS Sustainable Chem. Eng. 2019, 7, 16310−16319

N_2 gas with a 100 mL/min flow during the heating ramp. XRD was conducted using a Rigaku SmartLab XRD with Cu Kα radiation, and the X-rays were generated at 40 mA and 45 kV. The diffraction patterns were collected in the range of 5−55° 2θ with a step size of 0.02° 2θ. Mineral phases were identified using MDI Jade 2010. A Joel IT500 Scanning electron microscopy (SEM) was used for micromorphology observation in Secondary electron mode. Images were acquired on freshly fractured sections of the mortar bars. An accelerating voltage of 10 kV was chosen, and images were aquired with working distances of 11−13 mm and a magnification of 4000.

RESULTS AND DISCUSSION

Dimensional Stability. Dimensional stability was reflected by the evolution of longitudinal length of mortar bars (25 mm × 25 mm × 285 mm) measured during the 500 d study, as shown in Figure 3. The steam-cured mortars showed the highest expansion percentage at 500 d, an expected consequence of DEF. Mortar expansion commenced at ~250 d and rose to over 0.6% at 500 d. During the same storing period, expansion measured on the carbonation-cured mortar was consistently close to 0% and was substantially lower than that for the other three curing conditions used in this study and the ACI 318 length change requirement (0.1%). The high maximum curing temperature (85 °C) used for steam curing was to purposefully induce DEF and to verify the favorable binder chemistry and the timing of DEF. Therefore, the observation in Figure 3 suggests that carbonation curing leads to the highest dimensional stability at 500 d among the four curing regimes examined in this experiment.

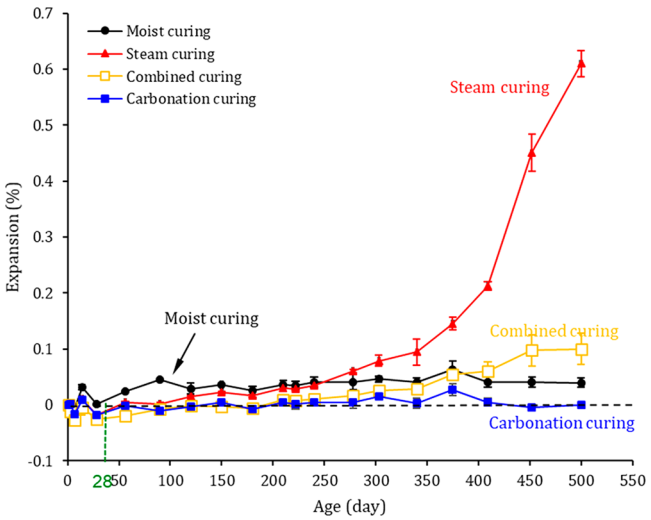

Figure 3. Evolution of longitudinal expansion of mortar bars after four different curing approaches. Steam-cured mortars show highest expansion, whereas carbonation curing leads to the most stable dimension during the measuring period of 500 d. This is conditional on the four curing protocols used in this study, due to the excessively high temperature designed for the steam curing to trigger DEF intentionally.

Expansion of the combined-cured mortar was close to that of the moisture-cured and carbonation-cured mortars until 400 d, but it subsequently displayed a slight uptick amounting to ~0.1% at 500 d. Additionally, the 500 d expansion of the combined-cured mortar was significantly lower than that of the steam-cured mortar, suggesting that DEF is potentially slowed down by the CO_2 carbonation.

The ettringite precipitation could cause microcracking even at unconstrained conditions due to crystallization stresses in the microstructure.[33] Figure 4 shows typical images capturing the surface appearance of mortar bars at 500 d. Cracks were clearly identified on the steam-cured specimens as shown in Figure 4b, whereas the other three groups displayed intact surfaces. Surface appearances of mortar bars agree with the expansion measurement given in Figure 3. Nevertheless, simple observation of mortar surface may not necessarily reflect possible occurrence of internal cracks, which would take a longer time to propagate externally. This was particularly true for mortars subjected to the combined curing, where the core region was less affected by carbonation, thus maintaining the chemical and mineral compositions similar to that of the typical steam-cured mortars.

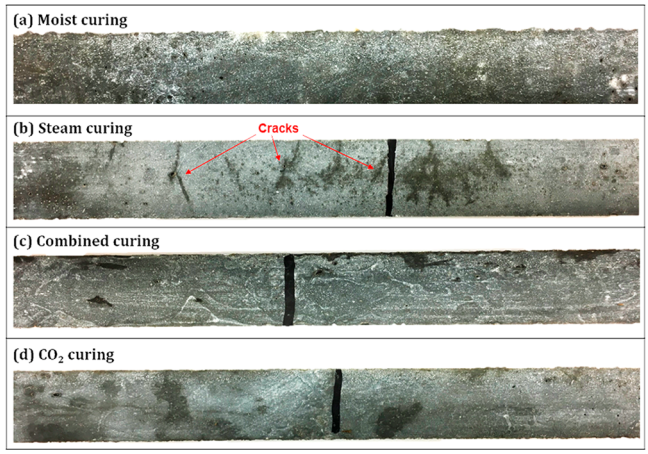

Figure 4. Surface observation of mortar bars after storing in saturated limewater for 500 d. Steam-cured mortars (at 85 °C maximum curing temperature) show visible cracks on surface.

Mass Gain. Mass gain of mortar bars can be attributed to three factors: (i) saturation of pores, particularly at early stages of storage, (ii) subsequent cement hydration, and (iii) formation of ettringite and/or AFm that takes up additional free water. All three factors are contributing to the postcuring mass gain of the steam-cured mortars. However, the impacts of factors (i) and (ii) appear less prominent as evidenced by the slow mass gain of the steam-cured sample shown in Figure 5. This is particularly valid for the first 28 d, essentially due to the high relative humidity and accelerated cement hydration induced by the steam curing process. The long-term formation of ettringite and AFm can potentially lead to an abrupt increase in mass, serving as a common indictor for the onset of DEF.[10,34] Figure 5 shows the mass gain of mortars subjected to the four curing conditions. For mortars subjected to moisture curing and combined curing, mass gain curves seemingly plateaued at ~250 d, whereas the steam-cured mortars transit to the induction period, in which cement hydration was almost complete and DEF had yet to be initiated. In general, it takes a longer period for DEF-induced expansion to appear on the mortar mass curves than for the mass gain of continuing cement hydration to level off. An induction period is therefore created in the steam-cured mortars. The mass gain of steam-cured mortars resumed at ~370 d, when significant expansion was simultaneously observed by the longitudinal length measurements depicted in Figure 3. The symptoms observed in mass and length of mortar bars collectively indicate the

DOI: 10.1021/acssuschemeng.9b03345
ACS Sustainable Chem. Eng. 2019, 7, 16310−16319

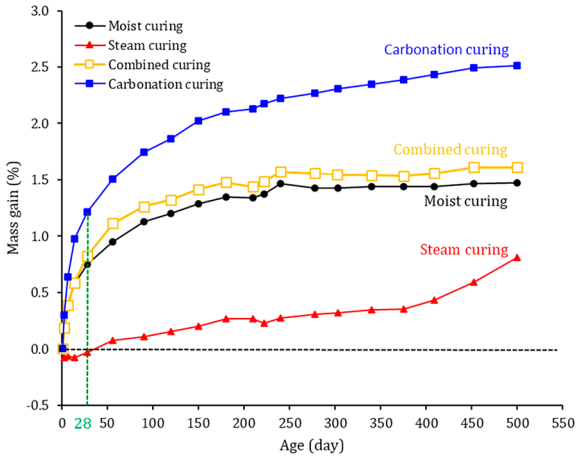

Figure 5. Evolution of mass of mortar bars after four different curing approaches.

occurrence of DEF in the steam-cured mortars. Another observation in Figure 5 was on the mass gain of carbonation-cured mortars, which continuously increased after 24 h and attained ~1.25% at 500 d. The mass gain of the carbonation-cured mortars is associated with the phase changes of Ms and ettringite, which are discussed in later sections.

Compressive Strength. Compressive strength was measured at 500 d and is shown in Figure 6. Carbonation-cured

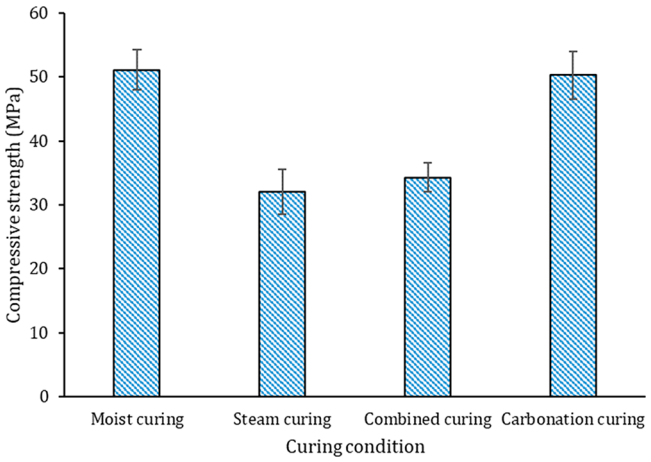

Figure 6. Compressive strength of mortars after storing in limewater for 500 d.

mortars achieved a compressive strength of 50 MPa, close to that of the moisture-cured reference (51 MPa). This trend is consistent with prior studies,[12,35] suggesting that the early age carbonation does not impede subsequent cement hydration that enables continuous strength gain in the long term. Steam curing, however, decreased the 500 d strength to 32 MPa, potentially due to two factors: (i) high temperature exposure at the early age tends to cause a thick layer of hydration products to form at the rim of unreacted cement grains, thus blocking the water supply for subsequent cement hydration[10] and (ii) microcracking caused by ettringite crystallization damages mechanical integrity that could decrease both strength and modulus.[36] These two factors were possibly valid for the core of the combined-cured mortars, which led to a similar strength reduction compared to the moisture-cured reference.

Water Absorption and Surface Electrical Resistivity. Water absorption was determined by recording the mass change of mortars from saturated to dry states by isothermally heating the samples. The chosen drying temperature can potentially impact this measurement. Although 105 °C is commonly used as the standard drying temperature for mortar and concrete,[37] mild drying at a lower temperature (~60 °C) is occasionally recommended to prevent microstructural damage induced by dehydration of metastable phases in the hydrated PC.[38,39] Figure 7 shows the water absorption results

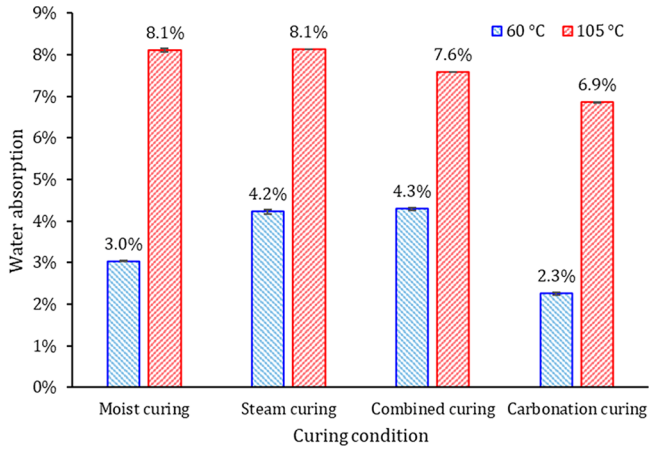

Figure 7. Water absorption of mortars after storing in limewater for 500 d. Water absorption was tested at two drying temperatures of 60 and 105 °C.

obtained by drying at 60 and 105 °C. Among the four batches, the carbonation-cured mortars displayed the lowest absorption at both temperatures. The low mortar absorption after carbonation curing is likely a consequence of the calcium carbonate precipitation in microporous space promoted by CO_2 carbonation. In reference to the masses obtained at 60 and 105 °C, the steam-cured mortars took up 4.2% and 8.1% water upon saturation, respectively. Steam curing increased the water absorption measured at 60 °C but did not lead to significant changes at 105 °C compared to the moisture-cured reference. This is mainly due to the chemical similarities between the steam-cured and moist-cured samples when partially dehydrated at 105 °C, as the short steam curing does not essentially alter cement chemical compositions at the early age. Additionally, the introduction of carbonation after steam curing (i.e., combined curing) slightly decreased the water absorption measured at 105 °C.

SER serves as an indicator for surface permeability of the mortar bars. Figure 8 describes the evolution of SER as a function of storing time in limewater. The moisture-cured reference displayed a slight uptick during 500 d as a result of subsequent PC hydration, whereas that of the steam-cured mortars displayed minimal changes after 28 d. The steam-cured mortar bars were also observed with the lowest SER, indicating that a more permeable mortar surface was created by the steam curing. The carbonation treatment of the steam-cured mortars was found to increase the SER, but not to the level of the moisture-cured reference. Additionally, carbonation curing led to a remarkably higher SER than the other curing methods. It is interesting that the SER of the carbonation-cured mortars followed a decreasing trend until 28 d and leveled off afterward. The SER measurement is essentially built

DOI: 10.1021/acssuschemeng.9b03345
ACS Sustainable Chem. Eng. 2019, 7, 16310−16319

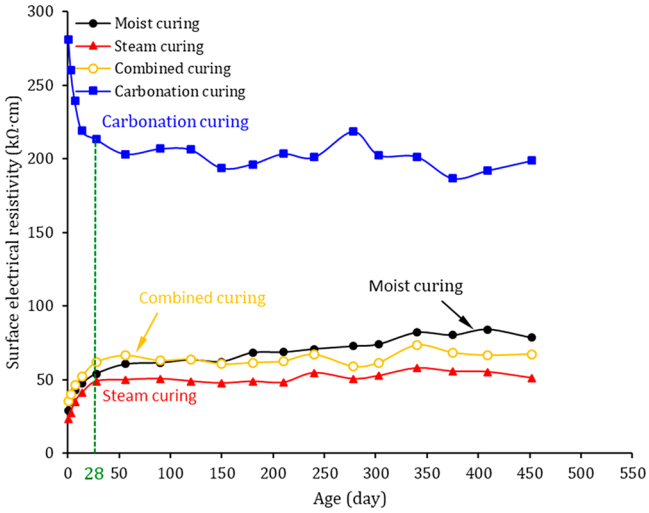

Figure 8. Evolution of surface electrical resistivity of mortar bars after four different curing approaches.

on closed electrical circuits formed in the porous space where water is present as a conducting media. The water loss associated with carbonation curing, however, created an unsaturated condition that restricted electrical conductance and increased electrical resistivity as a consequence. The water saturation process of carbonation-cured mortars after 24 h was potentially responsible for the decreasing SER until 28 d, when the specimens became saturated and achieved a high conductivity in the pore structure. The measurements of water absorption and surface resistivity collectively suggest that the CO_2 carbonation, whether applied with or without steam curing, is able to densify the long-term microstructures of PC mortars.

Thermogravimetric and X-ray Powder Diffraction Analyses. TGA and differential thermogravimetric analysis (DTG) supply insights into the assemblages of hydration and carbonation products in the mortar bars at 500 d. The DTG curves (Figure 9b) displayed the typical three-peak shape, corresponding to dehydration (30−300 °C), dehydroxylation (380−500 °C), and decarbonation (600−950 °C), respectively. Mass loss of each stage is graphically shown in Figure 9a and is listed in Table 2. Among the four curing regimes, carbonation curing displayed the lowest DTG intensity and mass loss associated with the dehydration stage. In reference to

Table 2. TGA Mass Loss (% Regulated to the Mass Ignited at 950 °C)

Temp range (°C)	Moist curing	Steam curing	Combined curing	Carbonation curing
30−300	16.9	15.3	13.4	11.9
380−500	5.0	5.3	3.9	1.8
600−950	4.1	3.4	9.3	14.9

the moisture-cured mortars, steam curing slightly decreased the dehydration mass loss from 16.9% to 15.3%, whereas the combined curing further decreased it to 13.4%. The profile of bound water in hydration products indicates that the formation of PC hydration products was reduced after CO_2 carbonation. The second observation by TGA/DTG relates to the mass loss associated with dehydroxylation, which was found to be lowest for the carbonation-cured mortars. The low dehydroxylation is indicative of low calcium hydroxide content and alkalinity. As such, carbonation curing potentially accentuates the vulnerability of reinforcing steel to corrosion when exposed to atmospheric carbonation. In the presence of supplementary cementitious materials (SCMs), the low alkalinity potentially impairs pozzolanic reaction, thereby resulting in lower mechanical integrity in the long term.[40] In contrast, the dehydroxylation mass loss of steam-cured specimens (i.e., 5.3%) appeared comparable to that of the moisture-cured reference (i.e., 5.0%).

Two key observations can be drawn from the decarbonation profile shown in Figure 9b. First, the $C\bar{C}$ precipitated through the early age carbonation (i.e., carbonation curing and combined curing) decomposed at a higher temperature than the limestone intermixed with OPC, as revealed by the moisture-cured mortars. This indicates that the CO_2-precipitated as calcium carbonate is chemically stable and the CO_2 sequestration enabled by carbonation curing is safe in the long term. Another observation was the two-step (or shoulder-shape) decarbonation identified in the DTG of carbonation-cured mortars, i.e., an additional decarbonation stage with a lower DTG intensity was formed at the temperature range of 500−650 °C prior to the main peak of $C\bar{C}$ decomposition (Figure 9b). This two-step decarbonation was also reported in previous studies, where it was attributed to the decomposition of metastable carbonates due to the carbonation of hydration products.[41] In particular, aragonite was identified as one of the products as a result of ettringite carbonation. Studies on

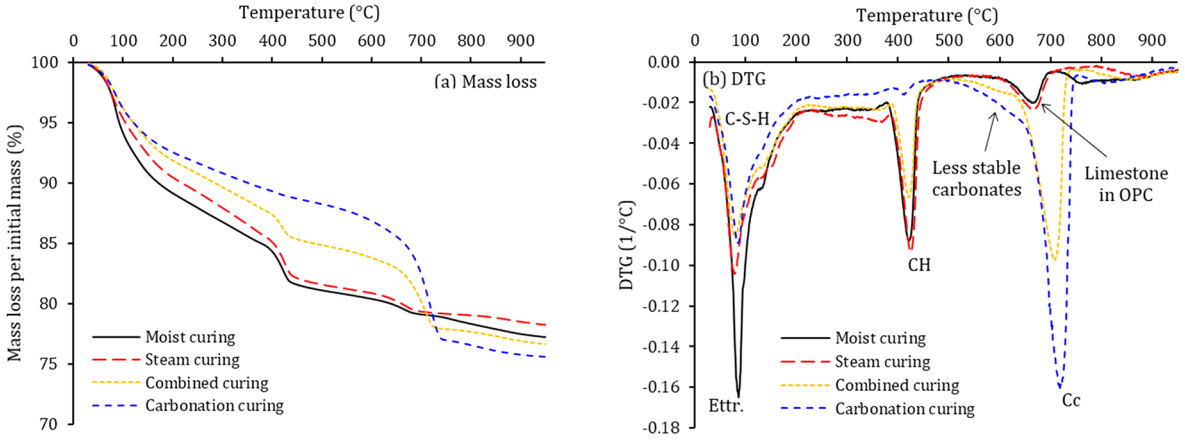

Figure 9. Thermogravimetric analysis results in forms of (a) mass loss and (b) differential thermogravimetric analysis.

DOI: 10.1021/acssuschemeng.9b03345
ACS Sustainable Chem. Eng. 2019, 7, 16310−16319

carbonation of calcium silicates[42] and partly hydrated PC[12] postulated the existence of amorphous $C\bar{C}$. It is likely that the metastable $C\bar{C}$ remains during the long-term postcarbonation hydration in the limewater condition.

Mineralogical compositions of mortar bars were examined using XRD. Calcite was clearly identified in the carbonation-cured and combined-cured mortars as shown in Figure 10.

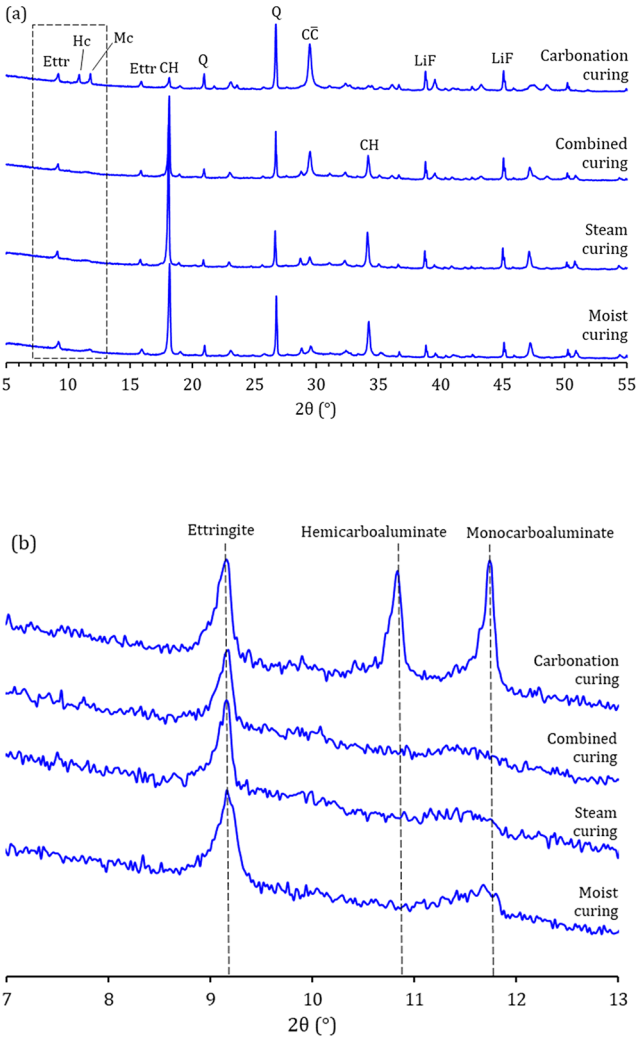

Figure 10. XRD pattern of mortar bars at (a) 5−55° 2θ showing whole pattern of mineral composition and (b) 7−13° 2θ showing local pattern of ettringite, hemicarboaluminate (Hc), and monocarboaluminate (Mc).

Portlandite was also identified in the carbonation-cured mortar but appeared at a lower intensity compared to that of other samples. The peak intensity corresponding to portlandite was consistent with dehydroxylation mass loss observed in the TGA results. Moreover, all mortars displayed noticeable peaks of ettringite regardless of the curing conditions. Figure 10b enlarges the XRD patterns in the range of 7−13° 2θ. The carbonation-cured mortars were found to form two distinct peaks, in addition to that of ettringite, corresponding to hemicarboaluminate ($C_4A\bar{C}_{0.5}H_{12}$, Hc) and monocarboaluminate ($C_4A\bar{C}H_{11}$, Mc), respectively. The relatively high background noises observed in the enlarged XRD patterns are due to the high magnitude and the overlapping of diffraction patterns of different mineral phases in the mixture. The small quantities and weak crystallinity of Hc and Mc are also responsible for the background noise. Mc was also identified in the moisture-cured reference but with a much lower intensity compared to that in the carbonation-cured mortars. It should be noted that the OPC used in this study was manufactured with about 5% intergrinded limestone, which potentially supplied the CO_3^{2-} source for Mc formation in the moisture-cured reference. In normal hydration of limestone-containing cement, Hc forms at an early age and progressively transforms to Mc after 7 d.[43] Excessive amounts of limestone offer an additional CO_3^{2-} source, thus potentially favoring formations of both Hc and Mc. The high intensities of Hc and Mc in the carbonation-cured specimens suggest that the carbonates precipitated during the early age carbonation likely participate in the postcarbonation hydration. In comparison, Mc/Hc was not obviously detected in the mortars subjected to steam curing or combined curing, indicating that the high temperature curing could hinder the $C\bar{C}$'s reaction in the long term.

Equations 6−8 list potential reactions of $C\bar{C}$ that may occur in mortars after carbonation curing. The anion exchange between CO_3^{2-} and SO_4^{2-} in Ms leads to the formations of Mc and Hc and releases $C\bar{S}$.[43] A high content of $C\bar{S}$ favors ettringite precipitation (eq 8), which might be responsible for the high moisture uptake in the carbonation-cured mortars over 500 d (see Figure 5). Interestingly, the limestone-sourced $C\bar{C}$ in the moisture-cured reference did not form similar quantities of Mc/Hc as that observed in the carbonation-cured mortars, as suggested by the diffraction intensity shown in Figure 10b. The cement used in this study comprised 5.2% limestone, which is sufficient for complete conversion of Al_2O_3 to Mc/Hc based on the stoichiometric calculation and chemical composition listed in Table 1. As such, we postulate that the $C\bar{C}$ precipitated by the early age carbonation appeared more favorable to facilitate reactions given by eqs 6 and 7, as opposed to the natural limestone present in OPC.

$$C_3A{\cdot}C\bar{S}{\cdot}H_{12}[Ms] + 0.5C\bar{C} \rightarrow C_3A{\cdot}0.5C\bar{C}{\cdot}H_{12}[Hc] + C\bar{S} \quad (6)$$

$$C_3A{\cdot}C\bar{S}{\cdot}H_{12}[Ms] + C\bar{C} \rightarrow C_3A{\cdot}C\bar{C}{\cdot}H_{11}[Mc] + C\bar{S} + H \quad (7)$$

$$C_3A{\cdot}C\bar{S}{\cdot}H_{12}[Ms] + 2C\bar{S} + 20H \rightarrow C_3A{\cdot}3C\bar{S}{\cdot}H_{32}\ [Ettringite] \quad (8)$$

Microstructure. Microstructure of mortars was observed using SEM to identify the micromorphology of ettringite. Figure 11a shows the typical microstructure formed in the steam-cured mortar at 500 d. Ettringite with typical acicular shapes was easily identified. Ettringite crystals appeared roughly 5−10 μm in length and were well dispersed in the microstructure. The identification of ettringite via SEM was consistent with the results of mortar length measurement (Figure 3) and surface cracking observation (Figure 4), which collectively confirm the occurrence of DEF in the steam-cured mortars. In mortars subjected to the combined curing, however, ettringite was hardly distinguishable. Figure 11b represents a typical location in the combined-cured mortar where ettringite could be visualized. Unlike the dispersed nature shown in Figure 11a, the ettringite "needle" appeared to have blunt edges and tended to form clusters in the unfilled pores. This clustered ettringite was potentially an onset of DEF, which could grow and eventually disperse in the microstructure if a longer storage was applied. A similar

DOI: 10.1021/acssuschemeng.9b03345
ACS Sustainable Chem. Eng. 2019, 7, 16310−16319

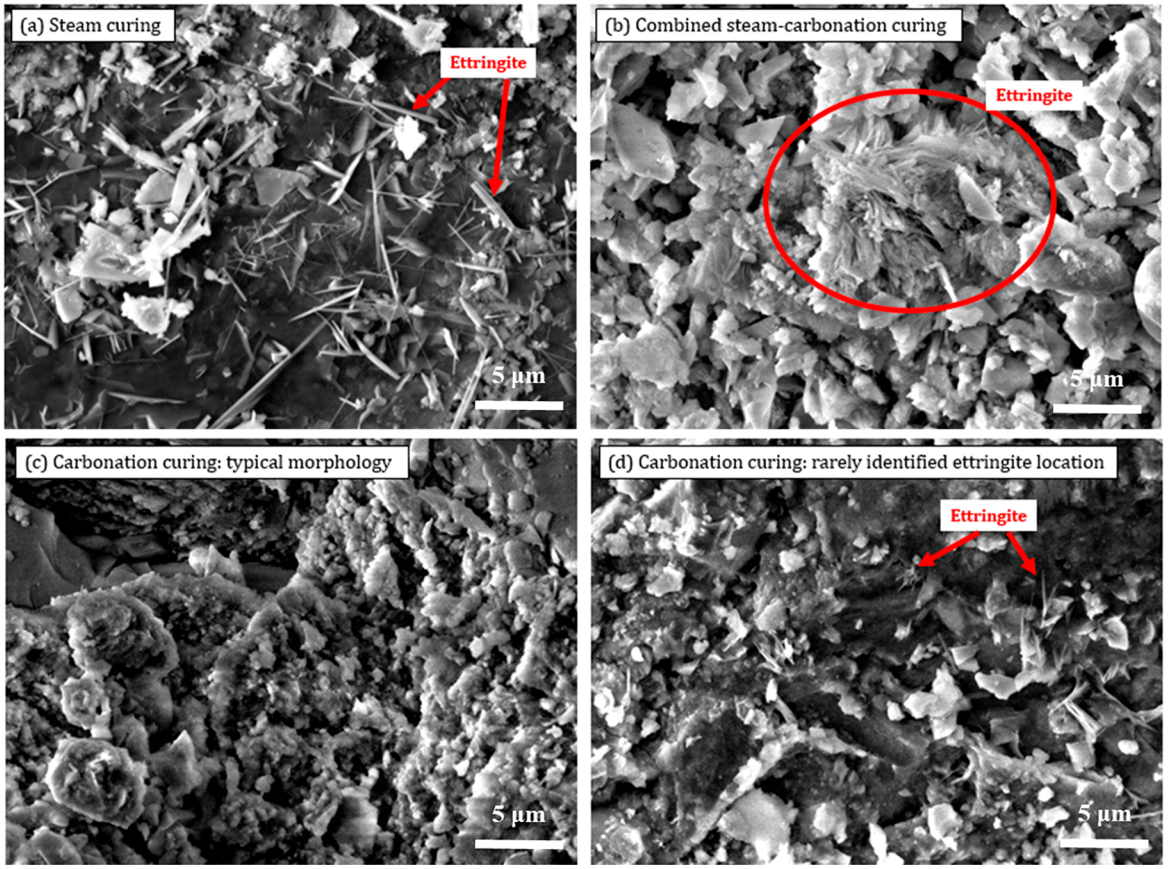

Figure 11. SEM images at 500 d for (a) typical morphology of mortar subjected to steam curing, (b) typical morphology of mortar subjected to combined steam-carbonation curing, (c) typical morphology of mortar subjected to carbonation curing, and (d) rarely identified ettringite location in mortar subjected to carbonation curing.

observation was reported by Tonsun and Baradan,[44] who identified the "ball ettringite" that filled up porous or cracked space in mortars but did not necessarily lead to expansion. However, the "ball ettringite" was suggested to continuously grow and eventually develop into the "needle ettringite" as typically observed in the steam-cured mortars. Ettringite in steam-cured PC-based materials is also recognized to reside in pores and voids at initial stages of DEF prior to dispersing elsewhere.[45] As such, it remains inconclusive whether combining carbonation with steam curing is capable of inhibiting the DEF-induced expansion, although the 500 d expansion can be substantially decreased.

The representative micromorphology of the carbonation-cured mortars is shown in Figure 11c, where ettringite was typically absent under magnification of ×4000. Calcite crystallites were not clearly observed in the carbonation-cured mortars, due to the intermixing with cement hydration products and their possible nanosize morphologies.[12] Figure 11d presents a rare location in which the acicular ettringite was identified. Nevertheless, the ettringite crystals were sparse and appeared shorter in length compared to those identified in the steam-cured mortars. The smaller crystal size and lower density ettringite were possibly responsible for the more stable geometry of the carbonation-cured mortars in the long term.

IMPLICATION FOR PRECAST INDUSTRY

The measurements of mortar bar length and compressive strength supply evidence that carbonation curing promotes long-term geometrical stability and mechanical integrity of PC-based materials. The findings of this research address the question as to whether the radical changes made by the intense CO_2 carbonation to the early age PC chemistry would adversely impact engineering properties of the materials with respect to the internal sulfate attack. Combining previous studies on the chemical resistance of carbonation-cured concrete,[14,15,46] we confirm the technical benefits added to PC-based materials by carbonation curing in the context of common environmental exposures, e.g., sulfate, acid, and chloride. The merits of carbonation curing also extend to the safe sequestration of CO_2, whereby waste CO_2 gas is converted into stable solid minerals that participate in the postcarbonation hydration process as well as enable the physical seeding effect as reported in a previous study.[18] Carbonation curing is a surface reaction (e.g., 3−4 mm reaction zone on a 25 mm square section in this study), as it creates a durable and chemically stable layer on the material surface. This surface effect might be partially altered in light of the combined steam-carbonation curing approach when scaled up to large applications but would maintain the enhanced dimensional stability of mortars cured only with carbonation. In industrial practice, the thickness of the carbonated layer, i.e., the depth of early age carbonation, could also be promoted as needed by tailoring material formulation, curing time, and CO_2 exposure conditions. It is recognized, however, that the pH reduction in the carbonation-cured materials remains a potential concern in the presence of steel reinforcements. Further investigations on corrosion resistance of steel reinforced concrete after carbonation curing are out of the scope of this study but are

DOI: 10.1021/acssuschemeng.9b03345
ACS Sustainable Chem. Eng. 2019, 7, 16310−16319

indispensable prior to its implementation. One must also note that the curing effectiveness (i.e., material early strength gain) would be prone to a size effect for carbonation curing but would appear more consistent for steam curing. For specimens with relatively large volume and small surface area, carbonation-cured materials may not develop early strength as high as that of as steam-cured ones, and therefore a slower early strength gain should be expected if steam curing is being simply substituted with carbonation curing. In this regard, the selection of an optimal curing approach would be informed by the specific needs and could potentially utilize a combined approach of carbonation and steam curing as reported in this study. Additional attention should also be paid to the adoption of low-concentration CO_2 gas for carbonation curing, particularly as it relates to industrial flue gas in which low carbonation efficiencies and the presence of sulfur might negate the technical benefits stated above. Beyond that, the early age CO_2 carbonation is a desirable precast curing approach, particularly in cases where chemical attacks are of primary concern to the longevity of materials.

CONCLUSIONS

The dimensional stability of mortars was examined with respect to four different curing conditions, including moist curing, steam curing (max temperature at 85 °C to purposefully induce DEF), carbonation curing, and combined steam-carbonation curing. The conclusions are listed below.

(1) Among the four curing approaches used in this study, carbonation curing demonstrates the most stable mortar geometry with ∼0% length change, whereas steam curing intentionally designed at an excessively high temperature leads to the highest expansion that attains over 0.6% at 500 days. The expansion of steam-cured mortars is substantially decreased to 0.1% by the application of CO_2 carbonation after the steam treatment.

(2) Ettringite is identified in all mortars at 500 days. Nevertheless, microscopic observation suggests that ettringite formed in the steam-cured mortars is well crystallized and dispersed, whereas ettringite observed in the mortars subjected to the combined steam-carbonation curing tends to cluster in local porous space. The uneven distribution and clustering morphology of ettringite after the combined steam-carbonation curing indicate the potential onset of DEF. Additionally, ettringite crystals appear sparse under the magnification of the carbonation-cured mortars.

(3) Calcium carbonate precipitated through carbonation curing does not act as an inert filler but rather acts as a reactive ingredient that promotes the formations of Mc and Hc. This phase transformation likely promotes ettringite formation and further densifies the microstructure of the carbonation-cured mortars. The transformation is also responsible for the high water uptake in the carbonation-cured mortars during the postcarbonation hydration.

AUTHOR INFORMATION

Corresponding Author

*Tel: +1-(734) 763-5470. E-mail: brellis@umich.edu.

ORCID

Duo Zhang: 0000-0003-1381-8162

Brian R. Ellis: 0000-0002-7253-4285

Notes

The authors declare no competing financial interest.

ACKNOWLEDGMENTS

Financial support for this work was provided by the U.S. Department of Energy, National Energy Technology Laboratory (NETL) through award No. DE-FE0030684.

CEMENT NOTATION:

C: CaO; S: SiO_2; A: Al_2O_3; F: Fe_2O_3; H: H_2O; $\bar{C}$: CO_2; $\bar{S}$: SO_3; Ms: monosulfoaluminate; Mc: monocarboaluminate; Hc: hemicarboaluminate

REFERENCES

(1) Zhou, Q.; Glasser, F. P. Thermal stability and decomposition mechanisms of ettringite at < 120 C. *Cem. Concr. Res.* **2001**, *31* (9), 1333−1339.

(2) Zhang, D.; Cai, X.; Hu, L. Effect of Curing Temperature on Hydration of Calcium Aluminate Cement−Calcium Sulfate−Limestone System. *J. Mater. Civ. Eng.* **2018**, *30* (9), No. 06018011.

(3) Collepardi, M. A state-of-the-art review on delayed ettringite attack on concrete. *Cem. Concr. Compos.* **2003**, *25* (4−5), 401−407.

(4) Stark, J.; Bollmann, K.Delayed ettringite formation in concrete. Nordic concrete research-publications: 2000, *23*, 4−28.

(5) Fu, Y.; Gu, P.; Xie, P.; Beaudoin, J. A kinetic study of delayed ettringite formation in hydrated Portland cement paste. *Cem. Concr. Res.* **1995**, *25* (1), 63−70.

(6) Taylor, H.; Famy, C.; Scrivener, K. Delayed ettringite formation. *Cem. Concr. Res.* **2001**, *31* (5), 683−693.

(7) Ahmad, S. Reinforcement corrosion in concrete structures, its monitoring and service life prediction−−a review. *Cem. Concr. Compos.* **2003**, *25* (4−5), 459−471.

(8) Black, L.; Garbev, K.; Gee, I. Surface carbonation of synthetic CSH samples: A comparison between fresh and aged CSH using X-ray photoelectron spectroscopy. *Cem. Concr. Res.* **2008**, *38* (6), 745−750.

(9) Suzuki, K.; Nishikawa, T.; Ito, S. Formation and carbonation of CSH in water. *Cem. Concr. Res.* **1985**, *15* (2), 213−224.

(10) Taylor, H. F. *Cement chemistry*. Thomas Telford: 1997, DOI DOI: 10.1680/cc.25929.

(11) Berger, R.; Young, J.; Leung, K. Acceleration of hydration of calcium silicates by carbon dioxide treatment. *Nature, Phys. Sci.* **1972**, *240* (97), 16−18.

(12) Rostami, V.; Shao, Y.; Boyd, A. J.; He, Z. Microstructure of cement paste subject to early carbonation curing. *Cem. Concr. Res.* **2012**, *42* (1), 186−193.

(13) Zhang, D.; Ghouleh, Z.; Shao, Y. Review on carbonation curing of cement-based materials. *Journal of CO2 Utilization* **2017**, *21*, 119−131.

(14) Zhang, D.; Shao, Y. Effect of early carbonation curing on chloride penetration and weathering carbonation in concrete. *Construction and Building Materials* **2016**, *123*, 516−526.

(15) Rostami, V.; Shao, Y.; Boyd, A. J. Durability of concrete pipes subjected to combined steam and carbonation curing. *Construction and Building Materials* **2011**, *25* (8), 3345−3355.

(16) Zhang, D.; Shao, Y. Surface scaling of CO2-cured concrete exposed to freeze-thaw cycles. *Journal of CO2 Utilization* **2018**, *27*, 137−144.

(17) Zhang, D.; Shao, Y. Enhancing chloride corrosion resistance of precast reinforced concrete by carbonation curing. *ACI Mater. J.* **2019**, *116* (3), 3−12.

(18) Zhang, D.; Li, V. C.; Ellis, B. R. Optimal pre-hydration age for CO2 sequestration through Portland cement carbonation. *ACS Sustainable Chem. Eng.* **2018**, *6* (12), 15976−15981.

DOI: 10.1021/acssuschemeng.9b03345
ACS Sustainable Chem. Eng. 2019, 7, 16310−16319

(19) Monkman, S. Maximizing carbon uptake and performance gain in slag-containing concretes through early carbonation. McGill University Montreal, QC, Canada, 2008.
(20) Kashef-Haghighi, S.; Ghoshal, S. CO2 sequestration in concrete through accelerated carbonation curing in a flow-through reactor. *Ind. Eng. Chem. Res.* **2010**, *49* (3), 1143−1149.
(21) El-Hassan, H.; Shao, Y.; Ghouleh, Z. Effect of Initial Curing on Carbonation of Lightweight Concrete Masonry Units. *ACI Materials Journal* **2013**, *110* (4), 441−450.
(22) Shao, Y.; Rostami, V.; He, Z.; Boyd, A. J. Accelerated carbonation of portland limestone cement. *J. Mater. Civ. Eng.* **2014**, *26* (1), 117−124.
(23) Divet, L.; Randriambololona, R. Delayed Ettringite Formation: The Effect of Temperature and Basicity on the Interaction of Sulphate and CSH Phase. *Cem. Concr. Res.* **1998**, *28* (3), 357−363.
(24) Ndiaye, K.; Cyr, M.; Ginestet, S. Durability and stability of an ettringite-based material for thermal energy storage at low temperature. *Cem. Concr. Res.* **2017**, *99*, 106−115.
(25) Nishikawa, T.; Suzuki, K.; Ito, S.; Sato, K.; Takebe, T. Decomposition of synthesized ettringite by carbonation. *Cem. Concr. Res.* **1992**, *22* (1), 6−14.
(26) Zhou, Q.; Glasser, F. Kinetics and mechanism of the carbonation of ettringite. *Adv. Cem. Res.* **2000**, *12* (3), 131−136.
(27) Xiantuo, C.; Ruizhen, Z.; Xiaorong, C. Kinetic study of ettringite carbonation reaction. *Cem. Concr. Res.* **1994**, *24* (7), 1383−1389.
(28) Kuzel, H.-J. Initial hydration reactions and mechanisms of delayed ettringite formation in Portland cements. *Cem. Concr. Compos.* **1996**, *18* (3), 195−203.
(29) Asamoto, S.; Murano, K.; Kurashige, I.; Nanayakkara, A. Effect of carbonate ions on delayed ettringite formation. *Construction and Building Materials* **2017**, *147*, 221−226.
(30) Al Shamaa, M.; Lavaud, S.; Divet, L.; Colliat, J. B.; Nahas, G.; Torrenti, J. M. Influence of limestone filler and of the size of the aggregates on DEF. *Cem. Concr. Compos.* **2016**, *71*, 175−180.
(31) Diamond, S. The relevance of laboratory studies on delayed ettringite formation to DEF in field concretes. *Cem. Concr. Res.* **2000**, *30* (12), 1987−1991.
(32) Safiuddin, M.; Hearn, N. Comparison of ASTM saturation techniques for measuring the permeable porosity of concrete. *Cem. Concr. Res.* **2005**, *35* (5), 1008−1013.
(33) Flatt, R. J.; Scherer, G. W. Thermodynamics of crystallization stresses in DEF. *Cem. Concr. Res.* **2008**, *38* (3), 325−336.
(34) Escadeillas, G.; Aubert, J.-E.; Segerer, M.; Prince, W. Some factors affecting delayed ettringite formation in heat-cured mortars. *Cem. Concr. Res.* **2007**, *37* (10), 1445−1452.
(35) Zhang, D.; Shao, Y. Early age carbonation curing for precast reinforced concretes. *Construction and Building Materials* **2016**, *113*, 134−143.
(36) Brunetaud, X.; Divet, L.; Damidot, D. Impact of unrestrained Delayed Ettringite Formation-induced expansion on concrete mechanical properties. *Cem. Concr. Res.* **2008**, *38* (11), 1343−1348.
(37) ASTM, C642−13, Standard test method for density, absorption, and voids in hardened concrete. In 2013; Vol. *4*, p 03, DOI DOI: 10.1520/C0642-13.
(38) Castro, J.; Bentz, D.; Weiss, J. Effect of sample conditioning on the water absorption of concrete. *Cem. Concr. Compos.* **2011**, *33* (8), 805−813.
(39) Gallé, C. Effect of drying on cement-based materials pore structure as identified by mercury intrusion porosimetry: a comparative study between oven-, vacuum-, and freeze-drying. *Cem. Concr. Res.* **2001**, *31* (10), 1467−1477.
(40) Zhang, D.; Cai, X.; Shao, Y. Carbonation curing of precast fly ash concrete. *J. Mater. Civ. Eng.* **2016**, *28* (11), No. 04016127.
(41) Auroy, M.; Poyet, S.; Le Bescop, P.; Torrenti, J.-M.; Charpentier, T.; Moskura, M.; Bourbon, X. Comparison between natural and accelerated carbonation (3% CO2): Impact on mineralogy, microstructure, water retention and cracking. *Cem. Concr. Res.* **2018**, *109*, 64−80.
(42) Goto, S.; Suenaga, K.; Kado, T.; Fukuhara, M. Calcium silicate carbonation products. *J. Am. Ceram. Soc.* **1995**, *78* (11), 2867−2872.
(43) Lothenbach, B.; Le Saout, G.; Gallucci, E.; Scrivener, K. Influence of limestone on the hydration of Portland cements. *Cem. Concr. Res.* **2008**, *38* (6), 848−860.
(44) Tosun, K.; Baradan, B. Effect of ettringite morphology on DEF-related expansion. *Cem. Concr. Compos.* **2010**, *32* (4), 271−280.
(45) Scrivener, K.; Taylor, H. Delayed ettringite formation: a microstructural and microanalytical study. *Adv. Cem. Res.* **1993**, *5* (20), 139−146.
(46) Rostami, V.; Shao, Y.; Boyd, A. J. Carbonation curing versus steam curing for precast concrete production. *J. Mater. Civ. Eng.* **2012**, *24* (9), 1221−1229.

DOI: 10.1021/acssuschemeng.9b03345
ACS Sustainable Chem. Eng. 2019, 7, 16310−16319